
The Effect of Undulations on the Electrostatic Potential in a Polyelectrolyte System

S. J. Miklavic

Phil. Trans. R. Soc. Lond. A 1994 **348**, 209-228

doi: 10.1098/rsta.1994.0089

Email alerting service

Receive free email alerts when new articles cite this article - sign up in the box at the top right-hand corner of the article or click [here](#)

To subscribe to *Phil. Trans. R. Soc. Lond. A* go to:

<http://rsta.royalsocietypublishing.org/subscriptions>

The effect of undulations on the electrostatic potential in a polyelectrolyte system

BY S. J. MIKLAVIC

*Departments of Physical Chemistry and Food Technology, Chemical Center,
University of Lund, Box 124, S-221 00 Lund, Sweden*

I consider the effect of macromolecular undulation on the electrostatic potential around a rod-like molecule. This effort is set to demonstrate the use of a particular perturbation technique through application to a geometrical system of general colloidal interest. The Poisson–Boltzmann equation together with a constant charge boundary condition on the well defined surface of an undulating cylinder is reformulated in integral equation form by use of Green’s theorem. A perturbation solution appropriate to the deformed boundary can be extracted when the Green function is approximated by that relevant to a reference, undeformed cylinder. Numerical results demonstrate that undulation causes significant deviations (increases) in electrochemical properties from expected behaviour, assuming rigid cylindrical symmetry. By considering the total free energy of the system it is found that electrostatics tend to diminish the extent of the undulations. The predicted deviations are briefly discussed in light of measured intermolecular electrostatic forces acting in a condensed phase of close-packed DNA. The perturbation technique has potential applications to mathematically similar problems occurring in hydrodynamics.

1. Introduction

In the theory of Gouy & Chapman (Verwey & Overbeek 1948), use of the Poisson–Boltzmann (PB) equation for the thermodynamical average, electrostatic potential gives quite a reliable description of the thermodynamic properties of electrically charged colloidal bodies in electrolyte suspensions. Comparisons made with more exact calculations (Wennerström *et al.* 1982; Carnie & Torrie 1984; Kjellander & Marcelja 1988) and even with direct experiment (Pashley 1981) have shown that only under extreme conditions does this mean-field description prove inadequate. With this overall confidence in its reliability one can then clearly point out the singular advantage that use of the PB equation has over higher order statistical mechanical theories: it allows for a simple examination of electrostatic properties of a charged system.

The PB equation has been solved to give the electrostatic potential and electrolyte distribution about and between a number of regularly shaped bodies: planes, spheres and cylinders (e.g. White 1977; Engström & Wennerström 1978; Bloomfield *et al.* 1980; Chan & Chan 1983; Vlachy & McQuarrie 1985; Sengupta & Papadopoulos 1992). Regular figures of equilibrium reduce the normally partial (nonlinear) differential equation to an ordinary (but still nonlinear) differential equation involving only the independent variable which describes the inhomogeneity of the

Phil. Trans. R. Soc. Lond. A (1994) **348**, 209–228

© 1994 The Royal Society

Printed in Great Britain

209

system. It is unfortunate, though, that even within this class the PB equation is rarely solvable analytically, the nonlinearity then often leading to difficulties in a subsequent numerical solution. Of course, dispensing with the assumption of regular shaped surfaces forces one, from the outset, to consider numerical techniques to obtain a solution (Gilson *et al.* 1987). Such intensive measures, though, bring to question the advantages of using the mean-field model at all.

Use of the PB equation together with the assumption of regular geometry has been ubiquitous in studies of surfactant aggregation, properties of biological cells and lipid vesicles, and those of linear biological macromolecules such as DNA and polypeptides. Given that these colloidal (e.g. surfactant phase structures) or biological (especially in the case of DNA and cells) macromolecules are rarely rigid, regularly shaped entities, it would be of some use to keep with the advantage of using the PB equation and still describe 'real' systems to the best approximation possible, even if the resulting description is then only qualitative. It is along this line of reasoning that perturbation theory becomes one obvious model.

It is the principal aim of this paper to demonstrate the use of a particular perturbation technique through its application to one geometrical system of general colloidal interest. The thermodynamic mean potential about an undulating cylindrical polyelectrolyte is obtained by solving the PB equation together with a constant charge boundary condition on the well-defined cylinder surface. The partial differential system can be reformulated in integral equation form by use of Green's theorem. A perturbation solution appropriate to the deformed boundary can be extracted when the Green function is approximated by that relevant to the reference, undeformed cylinder.

The circumstances of charged surfactant aggregates of the hexagonal phase (Jönsson & Wennerström 1987) and of linear biological macromolecules, such as DNA, induced to 'aggregate' into a condensed hexagonal array of aligned, close-packed molecules by application of an external osmotic stress (Maniatis *et al.* 1974; Rau *et al.* 1984), are largely responsible for the system chosen to simulate. This being a single cylindrical-like charged body confined within a cylindrical envelope of its near neighbours, that is, in the cell-model approximation (Hill 1956). The necessary impetus for the calculations presented below follows on from the efforts of others who have considered irregular shaped, charged surfaces. The recent work of Fogden *et al.* (1990) and Fogden & Ninham (1991) on undulating planar surfaces gave particular inspiration to the model developed here. Specifically, I give the macromolecule a small but well-defined, 'static' undulation in one direction transverse to the average axial direction. This allows me to invoke a perturbation treatment about the rigid cylinder case, using the amplitude as a perturbation parameter.

To my knowledge the work here is the first analytical attempt at a self-consistent electrostatic calculation in which the influence of at least one component mode of undulation of a charged cylindrical body is considered. In this context, however, the model has scope for further development to which I shall allude in the text. In more general review, despite the heavy accent on an electrochemical problem, the perturbation technique used has potential application to many mathematically similar problems occurring in hydrodynamics. This is timely with the increasing appearance of studies on potential flow about regularly shaped objects, cylinders in particular (Chew *et al.* 1992; Chau & Eatock-Taylor 1992) and to problems of secondary flow induced by the motion of solid bodies (Watson 1992). These studies

can obviously be generalized to include irregularly shaped boundaries to which perturbation theory can be applied.

In overview, the ideas are developed as follows. The next section introduces the problem to be solved. Section 3 provides reference solutions about which perturbations are performed. These are then described in §4. Some numerical results and a general discussion are left to the end.

2. Problem description

The image of the two-dimensional (2D) hexagonal array of aligned molecules, lends itself to a well defined representative model of a single molecule surrounded by a ‘wall’ of its neighbours. This can be further simplified by replacing these neighbours with a cylindrical boundary (see figure 1). This amounts to the application of the cell-model formalism (Marcus 1955; Hill 1956) in which a finite polyelectrolyte concentration of aligned molecules is converted into a free cellular volume allotted to each. In this case of average cylindrical symmetry, the cellular structure will have the same cylindrical geometry upon pre-averaging over the positions, relative phases and directions of undulation of neighbouring molecules, before the treatment of an individual. A radial parameter R , defines the extent of the cell and, implicitly the polyion concentration. Although this type of approach is quite common, the nature of the problem to be addressed here, concerning the effect of a well defined static undulation on the potential, provides a point of departure from usual treatments.

Let the macroion cross-sectional radius be denoted by a . It is assumed that the macromolecule has a uniform surface charge density σ , and that the uniformity is not disturbed by structural deformation. The surrounding electrolyte gives an ionic strength, $I = 2e^2c_0N_a 10^3$, defining an electrostatic screening length of $\lambda_D = \kappa^{-1}$, where

$$\kappa^2 = I/\epsilon\epsilon_0 k_B T, \quad (1)$$

where N_a is Avogadro’s number, c_0 is the bulk monovalent electrolyte concentration, e is the unit charge, ϵ_0 is the permittivity of free space, ϵ is the relative permittivity of the medium, k_B is Boltzmann’s constant, T is the temperature.

As outlined earlier, we use the mean electrostatic field model giving the potential, ψ , as the solution of the PB equation,

$$e\beta\nabla^2\psi(\mathbf{r}) = \kappa^2 \sinh(e\beta\psi(\mathbf{r})), \quad (2)$$

where ∇^2 is the laplacian operator and a Boltzmann distribution has been assumed for the charge distributions on the right-hand side. The coordinate system is such that the z -direction is along the axis of the right circular cylindrical cell (figure 1). Accompanying (2) are the boundary conditions which the potential, ψ , must satisfy: electroneutrality implies cell symmetry across the cell wall,

$$\partial\psi(\mathbf{r})/\partial r = 0, \quad \text{at } r = R \quad (3a)$$

and Gauss’ law at the macroion surface,

$$\partial\psi(\mathbf{r}_s)/\partial n = \sigma/\epsilon_0\epsilon. \quad (3b)$$

In this expression the operator $\partial/\partial n$ denotes differentiation along the outward normal from the region, i.e. inwards over the inner cylinder toward the origin. \mathbf{r}_s denotes the position vector on the surface of the inner cylinder.

Any undulations of a flexible macromolecule can be represented by or decomposed

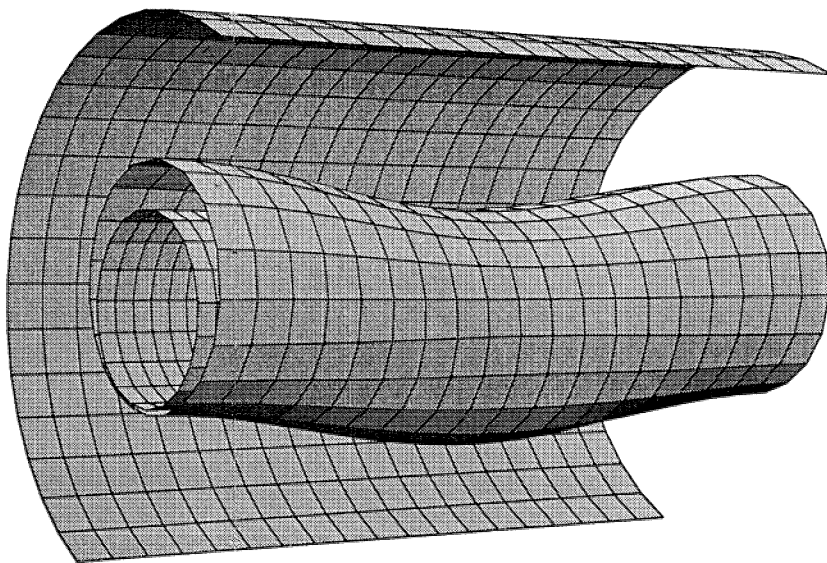


Figure 1. Schematic of the deformed polyelectrolyte molecule of radius a and centreline undulation, $\alpha \cos(kz)$, confined within a right cylindrical shell of radius R . Within the undulating molecule is the reference cylinder of radius $r_0 = a - \alpha$.

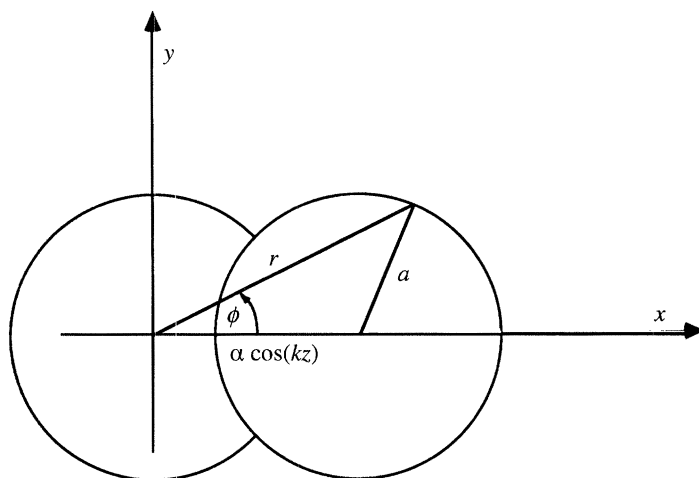


Figure 2. A cross-section view of the charged macromolecule in its unperturbed and its perturbed configuration (greatly exaggerated). The polar and cartesian coordinate system is defined here.

into an infinite sum of Fourier modes, but to simplify the analysis one can, like Fogden and co-workers (Fogden *et al.* 1990; Fogden & Ninham 1991), single out one mode of undulation as dominant. The centre line of the polyelectrolyte is given a cosinusoidal displacement of amplitude α and wavelength $\lambda = 2\pi/k$ in the x -direction: $x = \alpha \cos(kz)$ (although, in general, one should have to supplement this term by cosines and sines of multiples of kz , in a full series representation). Application of simple trigonometry (figure 2) leads to the equation for the surface of the macroion, $S(r, \phi, z)$:

$$S(r, \phi, z) = r - a\{\eta \cos(kz) \cos(\phi) + \sqrt{[1 - \eta^2 \cos^2(kz) \sin^2(\phi)]}\} = 0. \quad (4)$$

Values of α and k , representative of the undulation, are assumed small. In (4), $\eta = \alpha/a$. I mention here that, from 2D isotropy, all molecules would presumably have the same fluctuation mode but, from entropic considerations, they have random phases. In this case the unlikelihood of any two neighbours undulating in phase gives substance to the first order approximation that the confining cell be unperturbed.

The nonlinearity of (2) and the full three-dimensionality of the system implied by the inner boundary prevent a straightforward means of obtaining a solution. However, for those cases where the electrostatic potential, ψ , is small everywhere (i.e. $|\psi|$ of about $k_B T/e$) the behaviour of ψ is acceptably described by the linear PB equation,

$$\nabla^2 \psi(\mathbf{r}) - \kappa^2 \psi(\mathbf{r}) = 0. \quad (5)$$

Fortunately, for the DNA system which is implicitly considered, the amount of salt normally present together with the combined features of ion binding and counterion condensation, both of which effectively neutralize the DNA charge by a factor of $100(1-f) \approx 70-90\%$ (Bloomfield *et al.* 1980), mean that this criterion may not be difficult to meet. In the numerical examples to follow, σ is taken as a product of the bare charge expected on DNA, $1/2\pi a\zeta$, with ζ being the distance between charge bearing phosphates along the macroion (about 1.7 Å, where 1 Å = 10^{-1} nm), and the factor f termed (by Manning (1978) and Bloomfield (1991)) a residual charge fraction after counterion condensation, here set equal to 0.11, 0.24 and 0.5. The first two values have been determined for divalent and monovalent electrolyte solutions, respectively (although we only treat the latter case explicitly). The third case is not intended to have any specific bearing on any one system but is mentioned only for illustrative purposes.

Equation (5) with boundary conditions (3) at the cell wall and inner surface (4) are to be solved and ψ is then used in determination of thermodynamic quantities.

In the most familiar case where the polyelectrolyte surface is assumed to be a rigid right cylinder, equations (3) to (5) expressed in cylindrical polar coordinates would be a separable system. In the present case, even though the differential equation remains separable in cylindrical polar coordinates, the inner boundary prevents the total separability of the problem. I proceed to an approximate solution by means of perturbation theory in §4. For comparison and point of departure I first present solutions to the unperturbed problem.

3. Reference solutions

The undisturbed case has the polyion surface simply given, defined by $r = r_0$, say. From axial symmetry, the corresponding potential, ψ_0 , is then independent of ϕ and z coordinates, and the partial differential equation, (5), reduces to an ordinary differential equation in the radial variable,

$$\frac{1}{r} \frac{d}{dr} \left(r \frac{d\psi_0}{dr} \right) - \kappa^2 \psi_0 = 0. \quad (6)$$

The boundary condition (3*b*) is similarly simplified:

$$d\psi_0/dr = -\sigma/\epsilon\epsilon_0.$$

The solution of the modified Helmholtz equation, (6), can readily be expressed in

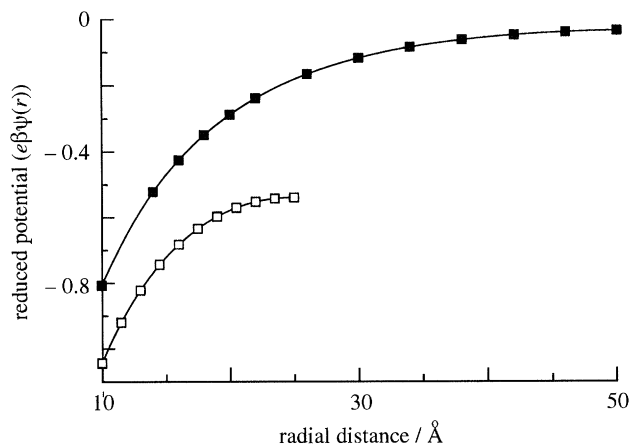


Figure 3. Electrostatic potential in reduced units ($e\beta\psi$) in the unperturbed condition, as a function of radius. Both curves correspond to an inner cylinder radius of 10 \AA . Two different cell radii are considered: $R = 50 \text{ \AA}$ (\blacksquare) and $R = 25 \text{ \AA}$ (\square). Here, and in subsequent figures (unless otherwise stated), $\sigma = -1.65 \times 10^{-2} \text{ C m}^{-2}$ and $c_0 = 0.05 \text{ M}$ and $\lambda = 20 \text{ \AA}$.

terms of zero order modified or hyperbolic Bessel functions (Morse & Feshbach 1953; Abramowitz & Stegun 1968), I_0, K_0 :

$$\psi_0(r) = -\frac{\sigma}{\epsilon\epsilon_0\kappa} \frac{[I_0(\kappa r)K'_0(\kappa R) - K_0(\kappa r)I'_0(\kappa R)]}{[I_0(\kappa r_0)K'_0(\kappa R) - K_0(\kappa r_0)I'_0(\kappa R)]}$$

Although I have not been able to find this explicit solution for the cell-model problem quoted in the literature, the solution of (6) for the case of an isolated cylinder is rather well documented (Brenner & Parsegian 1974; Schellman & Stigter 1977; Stigter 1978). The solution above is likewise straightforward to obtain. Figure 3 shows a plot of ψ_0 as a function of r between the cylindrical boundaries for two different cell radii.

The perturbation method adopted below requires consideration of the Green function for this same problem. The equation satisfied by the Green function, G_κ , is again the modified Helmholtz equation, now with a point source:

$$\nabla^2 G_\kappa(\mathbf{r}, \mathbf{r}') - \kappa^2 G_\kappa(\mathbf{r}, \mathbf{r}') = -4\pi\delta(\mathbf{r} - \mathbf{r}'). \quad (7)$$

The convention of ascribing homogeneous Neumann conditions to G_κ corresponding to the inhomogeneous Neumann conditions satisfied by ψ , is followed. The usual procedure of solving (7) with the given boundary conditions is to express G_κ as an eigenfunction expansion involving sums of products of the eigenfunctions of the separable coordinates (Morse & Feshbach 1953). In cylindrical polar coordinates,

$$G_\kappa(\mathbf{r}, \mathbf{r}') = \frac{1}{(2\pi)^2} \sum_m \int_{-\infty}^{\infty} dp \exp(ip(z-z')) \exp(im(\phi-\phi')) Q_{mp}(r, r'). \quad (8)$$

The index m is constrained to be an integer from periodicity whereas for an infinite right cylinder, p is a continuous variable. The function $Q_{mp}(r, r')$ is to be determined. The delta function on the right-hand side of (7) has the following expansion in these coordinates:

$$\delta(\mathbf{r} - \mathbf{r}') = \frac{1}{(2\pi)^2} \sum_{m=-\infty}^{\infty} \exp(im(\phi-\phi')) \int_{-\infty}^{\infty} dp \exp(ip(z-z')) \frac{\delta(r-r')}{r'}. \quad (9)$$

Inserting this into (7), multiplying by $\exp(-iqz)$ and $\exp(-in\phi)$ and integrating over the variable ranges $z \in (-\infty, \infty)$ and $\phi \in [0, 2\pi]$ leads to an inhomogeneous Bessel equation for $Q_{mp}(r, r')$,

$$\frac{1}{r} \frac{d}{dr} \left(r \frac{dQ_{mp}}{dr} \right) - \left(\gamma_p^2 + \frac{m^2}{r^2} \right) Q_{mp} = -4\pi \frac{\delta(r-r')}{r'},$$

with $\gamma_p^2 = \kappa^2 + p^2$. The solution satisfying boundary conditions and the jump discontinuity in the derivative of Q across $r = r'$, which gives rise to the delta function source, is

$$Q_{mp}(r, r') = \frac{-4\pi}{r' W(q^{(1)}, q^{(2)})} q^{(1)}(r_{<}) q^{(2)}(r_{>}), \quad (10)$$

where $r_{<}(r_{>})$ takes the value of r or r' , depending on which takes on the lesser (greater) value. $q^{(1)}$ and $q^{(2)}$ are two linearly independent solutions of the homogeneous differential equation adjusted to satisfy the homogeneous boundary conditions at r_0 and R respectively,

$$\left. \begin{aligned} q^{(1)}(r) &= I_m(\gamma_p r) K'_m(\gamma_p r_0) - K_m(\gamma_p r) I'_m(\gamma_p r_0), \\ q^{(2)}(r) &= I_m(\gamma_p r) K'_m(\gamma_p R) - K_m(\gamma_p r) I'_m(\gamma_p R). \end{aligned} \right\} \quad (11)$$

The wronskian of the two solutions, $W(q^{(1)}, q^{(2)})$, evaluated at r' , provides the correct normalization. Inserting (11) into $W(q^{(1)}, q^{(2)})$,

$$W(q^{(1)}, q^{(2)}) = q^{(1)}(x) (q^{(2)}(x))' - q^{(2)}(x) (q^{(1)}(x))', \quad \text{at } x = r',$$

performing the indicated derivatives, expanding the products and recollecting terms will show that W can be rewritten as

$$W(q^{(1)}, q^{(2)}) = \gamma_p W(I_m, K_m) \Delta_{mp},$$

where (Arfken 1970)

$$W(I_m, K_m) = I_m(x) K'_m(x) - K_m(x) I'_m(x) = -1/x \quad (12)$$

is the wronskian for the hyperbolic Bessel functions of order m , $I_m(x)$ and $K_m(x)$, and

$$\Delta_{mp} = I'_m(\gamma_p r_0) K'_m(\gamma_p R) - I'_m(\gamma_p R) K'_m(\gamma_p r_0) \quad (13)$$

is a factor independent of the variable r' , depending only on the inner and outer limits, r_0 and R .

Thus, the solution (10), becomes

$$Q_{mp}(r, r') = \frac{4\pi}{\Delta_{mp}} q^{(1)}(r_{<}) q^{(2)}(r_{>}). \quad (14)$$

The connection between the Green function, (8) with (14), and my earlier solution for ψ_0 is made through Green's theorem:

$$\psi(\mathbf{r}) = \frac{1}{4\pi} \int_{S_1+S_0} G_\kappa(\mathbf{r}, \mathbf{r}') \nabla_{\mathbf{r}'} \psi(\mathbf{r}') \cdot d\mathbf{s} - \frac{1}{4\pi} \int_{S_1+S_0} \psi(\mathbf{r}') \nabla_{\mathbf{r}} G_\kappa(\mathbf{r}, \mathbf{r}') \cdot d\mathbf{s}, \quad (15)$$

where $S_1 + S_0$ denotes the total surface enclosing the volume interior (the annular region bounded between the inner and outer cylinders). In these integrals, \mathbf{r}' denotes the source point on the surface of one of the two cylinders. The elements of surface area, $d\mathbf{s}$, are directed away from the interior volume. Equation (15) forms the basis

for an approximate solution to the undulating polyion problem. For the moment, with the respective Neumann boundary conditions on G_κ and ψ_0 on the inner and outer surfaces, (15) reduces to

$$\psi_0(\mathbf{r}) = \frac{1}{4\pi} \int_{S_1} \frac{\sigma}{\epsilon\epsilon_0} G_\kappa(\mathbf{r}, \mathbf{r}') ds,$$

where for a uniform surface charge distribution, all the ϕ' and z' integrals vanish from symmetry, except the case of $p = m \equiv 0$. Setting $r_0 = a$ and again using property (12) on $q^{(1)}$ in (11) leads to my earlier expression for ψ_0 .

4. The perturbed problem

With the sinusoidal z dependence of the centre line, leading to (4) for the equation of the surface, the boundary condition, (3b),

$$\nabla S \cdot \nabla \psi = |\nabla S| \sigma / \epsilon\epsilon_0 \quad (16)$$

with (5) results in a non-separable partial differential system. To avoid solving the differential problem directly (if it were possible) we proceed along an alternative approximate, but more direct, route suggested in Morse & Feshbach (1953), based on the integral equation (15). Were one in possession of the appropriate exact Green function for the perturbed boundary, then (15) would have led to as simple an integral representation as for the above rigid cylinder case. Instead, we take the approximate step of using the Green function given by (8) together with (14) which satisfies the same differential equation and appropriate homogeneous boundary conditions but only when evaluated on the surface of a rigid, reference cylinder of some radius, $r_0 \leq a - \alpha$. In such a circumstance the volume of validity of this Green function contains the real volume of our interest although the eigenfunctions of the expansion are no longer orthonormal when restricted to the perturbed region. The practical price to pay is that, with this G_κ , the second term of (15) does not vanish identically, but instead one has an inhomogeneous integral equation to solve.

In preparation for the outlined task, the expression for G_κ in (8) needs to be modified to be consistent with the case of a periodic z -structure. The z contribution to the delta function in (9) should be replaced by the expression corresponding to a periodic generalized function,

$$\delta(z - z') = \frac{k}{2\pi} \sum_{p=-\infty}^{\infty} \exp(ipk(z - z')),$$

having the same periodicity, $2\pi/k$, as the cylinder undulation. Thus,

$$G_\kappa(\mathbf{r}, \mathbf{r}') = \frac{k}{(2\pi)^2} \sum_p \epsilon_p \cos(pk(z - z')) \sum_m \epsilon_m \cos(m(\phi - \phi')) Q_{mp}(r, r'), \quad (17)$$

with $\epsilon_{p(m)} = 1$ if $p(m) = 0$, and 2 otherwise. $Q_{mp}(r, r')$ is unchanged except that p in (14) and in the expression for γ_p is replaced by pk , with p now an integer.

Further identifications are necessary. The boundary shape has the following expansion:

$$S(r, \phi, z) = r - a - aF(\phi, z), \quad (18a)$$

$$\text{with } F(\phi, z) = \eta \cos(kz) \cos(\phi) - \sum_{n=1}^{\infty} \left[\frac{1}{2} \right] \eta^{2n} \cos^{2n}(kz) \sin^{2n}(\phi). \quad (18b)$$

In addition, for any function φ (in our case G_κ or ψ),

$$\nabla\varphi(\mathbf{r}) \cdot \mathbf{ds} = \frac{\partial\varphi}{\partial n} \mathbf{ds} = \left(\frac{\partial\varphi}{\partial r} - \frac{a}{r^2} \frac{\partial\varphi}{\partial\phi} \frac{\partial F}{\partial\phi} - a \frac{\partial\varphi}{\partial z} \frac{\partial F}{\partial z} \right) r \, d\phi \, dz, \quad (19)$$

which is to be evaluated on the surface $S(r, \phi, z)$. Condition (16) becomes

$$\frac{\partial\psi}{\partial n} \mathbf{ds} = \frac{\sigma}{\epsilon\epsilon_0} |\nabla S| r \, d\phi \, dz, \quad (20)$$

where, to third order in η ,

$$|\nabla S| = 1 + \frac{1}{2}\eta^2 [(ka)^2 \sin^2(kz) \cos^2(\phi) + (a/r)^2 \cos^2(kz) \sin^2(\phi)] \\ + \eta^3 \cos(kz) \cos(\phi) \sin^2(\phi) [(a/r)^2 \cos^2(kz) - (ka)^2 \sin^2(kz)]. \quad (21)$$

The remaining explicit and implicit r dependence in (19)–(21) can be eliminated by appeal to (18) and to the following expansion (also given to third order):

$$(a/r)^2 = 1 - 2\eta \cos(kz) \cos(\phi) + \eta^2 \cos^2(kz) [\sin^2(\phi) + 3 \cos^2(\phi)] \\ - \eta^3 \cos^3(kz) [4 \cos^3(\phi) + 3 \sin^2(\phi) \cos(\phi)]. \quad (22)$$

Expressions for $\partial F/\partial\phi$ and $\partial F/\partial z$ also follow directly from (18*b*). The partial derivatives of G_κ , which are needed when G_κ is substituted in (19) in place of φ , are equally straightforward from (14) and (17).

In view of G_κ being approximate, (15) remains a full integral equation which can in principle be solved to any desired order by successive substitution/iteration. What is immediately apparent is that with each substitution (and integral to be evaluated) the r' argument of Q_{mp} must be replaced by $a + aF(\phi', z')$, introducing a convoluted perturbation expansion/integration procedure. What is anticipated, and confirmed numerically later, is that for small α and k one need only explicitly consider the first iterate solution.

The eventual function must reflect the periodicity and symmetry of the perturbation: periodic in ϕ and z ; symmetric about $\phi = 0$ and $z = 0$; and ‘cross-periodicity’, $\psi(r, \phi, z) = \psi(r, \phi + \pi, z + \frac{1}{2}\lambda)$. As is common with perturbation expansions, successively higher orders of η bring in higher order harmonics of the fundamental, giving ever finer detail to the solution. In fact it can be established from the prescription below that periodicity and symmetry can be preserved by terms of odd order of η containing combinations of odd harmonics up the power of η , and likewise by terms of even orders involving combinations of even harmonics. Considering, in turn, the inhomogeneous term as a zero order approximation ($i = 0$) and first iterate as a first order correction ($i = 1$), the potential from either has the form

$$\psi^{(i)} = f_1^{(0)}(r) + \eta f_1^{(1)}(r) \cos(kz) \cos(\phi) + \eta^2 (f_1^{(20)}(r) + f_1^{(21)}(r) \cos(2\phi) \\ + f_1^{(22)}(r) \cos(2kz) + f_1^{(23)}(r) \cos(2kz) \cos(2\phi)) + O(\eta^3). \quad (23)$$

The inhomogeneous term,

$$\psi^{(0)}(\mathbf{r}) = \frac{\sigma}{4\pi\epsilon\epsilon_0} \frac{k}{(2\pi)^2} \sum_{m,p} \epsilon_m \epsilon_p \int_0^{2\pi/k} dz' \int_0^{2\pi} d\phi' \cos(m(\phi - \phi')) \cos(pk(z - z')) \\ \times \{Q_{mp}(r, r') |\nabla S| r'\}_{S(r', \phi', z')}, \quad (24)$$

can be evaluated approximately by means of expansion (18) for r' , (21) for $|\nabla S|$, and by using a Taylor series expansion of $Q_{mp}(r, a + aF(\phi', z'))$ in η (or equivalently α):

$$Q_{mp}(r, a + aF(\phi, z)) = \sum_n \frac{\eta^n}{n!} Q_{mp}^{(n)}(r, a; \phi, z),$$

with

$$Q_{mp}^{(n)} = \left(\frac{\partial^n}{\partial \eta^n} Q_{mp} \right) \Big|_{\eta=0},$$

where the ϕ and z dependence is now external to the Bessel functions. Written explicitly, the first few terms are

$$Q_{mp}^{(0)} = 4\pi \frac{S_0^{(mp)}(r) T_0^{(mp)}(a)}{\Delta_{mp}},$$

$$Q_{mp}^{(1)} = 4\pi \frac{S_0^{(m)}(r) T_1^{(mp)}(a)}{\Delta_{mp}} (\gamma_p a) \cos(kz') \cos(\phi')$$

and

$$Q_{mp}^{(2)} = 4\pi \frac{(\gamma_p a) S_0^{(mp)}(r)}{\Delta_{mp}} [(\gamma_p a) T_2^{(mp)}(a) \cos^2(\phi') - T_1^{(mp)}(a) \sin^2(\phi')] \cos^2(kz'),$$

where Δ_{mp} is defined by (13) and

$$\left. \begin{aligned} T_0^{(mp)}(x) &\equiv q^{(1)}(x) = I_m(\gamma_p x) K'_m(\gamma_p r_0) - K_m(\gamma_p x) I'_m(\gamma_p r_0), \\ T_n^{(mp)}(x) &= I_m^{(n)}(\gamma_p x) K'_m(\gamma_p r_0) - K_m^{(n)}(\gamma_p x) I'_m(\gamma_p r_0), \\ S_0^{(mp)}(x) &\equiv q^{(2)}(x) = I_m(\gamma_p x) K'_m(\gamma_p R) - K_m(\gamma_p x) I'_m(\gamma_p R), \\ S_n^{(mp)}(x) &= I_m^{(n)}(\gamma_p x) K'_m(\gamma_p R) - K_m^{(n)}(\gamma_p x) I'_m(\gamma_p R). \end{aligned} \right\} \quad (25)$$

Superscripts on the Bessel functions denote differentiations. With all these expansions in place, multiplication, recollection of terms of powers of η and straightforward evaluation of the z' and ϕ' integrals results in only the $m = p = 0$ term surviving at zero order; the $m = p = 1$ term surviving at order η ; the $m, p = 0, 2$ terms surviving at order η^2 ; $m, p = 1, 3$ surviving at order η^3 , etc. To second order, one arrives at the following expressions for the coefficients of (23):

$$f_0^{(0)}(r) = \frac{\sigma a T_0^{(00)}(a) S_0^{(00)}(r)}{\epsilon \epsilon_0 \Delta_{00}}, \quad (26a)$$

$$f_0^{(1)}(r) = \frac{\sigma a ((\gamma_1 a) T_1^{(11)}(a) + T_0^{(11)}(a)) S_0^{(11)}(r)}{\epsilon \epsilon_0 \Delta_{11}}, \quad (26b)$$

$$\left. \begin{aligned} f_0^{(20)}(r) &= \frac{\sigma a}{\epsilon \epsilon_0} ((\gamma_0 a)^2 T_2^{(00)}(a) + (\gamma_0 a) T_1^{(00)}(a) + (ka)^2 T_0^{(00)}(a)) \frac{S_0^{(00)}(r)}{8\Delta_{00}}, \\ f_0^{(21)}(r) &= \frac{\sigma a}{\epsilon \epsilon_0} ((\gamma_0 a)^2 T_2^{(02)}(a) + 3(\gamma_0 a) T_1^{(02)}(a) + (ka)^2 T_0^{(02)}(a)) \frac{S_0^{(02)}(r)}{8\Delta_{02}}, \\ f_0^{(22)}(r) &= \frac{\sigma a}{\epsilon \epsilon_0} ((\gamma_2 a)^2 T_2^{(20)}(a) + (\gamma_2 a) T_1^{(20)}(a) - (ka)^2 T_0^{(20)}(a)) \frac{S_0^{(20)}(r)}{8\Delta_{20}}, \\ f_0^{(23)}(r) &= \frac{\sigma a}{\epsilon \epsilon_0} ((\gamma_2 a)^2 T_2^{(22)}(a) + 3(\gamma_2 a) T_1^{(22)}(a) - (ka)^2 T_0^{(22)}(a)) \frac{S_0^{(22)}(r)}{8\Delta_{22}}. \end{aligned} \right\} \quad (26c)$$

One iteration involving the homogeneous term in (15) represents a first order correction to the above; for convenience this will be denoted by $\Delta\psi^{(1)}(\mathbf{r})$. From (19) we get

$$\begin{aligned} \Delta\psi^{(1)}(\mathbf{r}) = & \frac{1}{4\pi} \frac{k}{(2\pi)^2} \sum_{m,p} \epsilon_m \epsilon_p \int_0^{2\pi/k} dz' \int_0^{2\pi} d\phi' \left\{ \psi(r', \phi', z') \right. \\ & \times \left[\cos(pk(z-z')) \cos(m(\phi-\phi')) \frac{\partial Q_{mp}(r, r')}{\partial r'} \right. \\ & - \frac{a}{r'^2} m \cos(pk(z-z')) \sin(m(\phi-\phi')) Q_{mp}(r, r') \frac{\partial F}{\partial \phi'} \\ & \left. \left. - apk \sin(pk(z-z')) \cos(m(\phi-\phi')) Q_{mp}(r, r') \frac{\partial F}{\partial z'} \right] r' \right\}_{S(r', \phi', z')}. \quad (27) \end{aligned}$$

Insertion of a suitable estimate for $\psi(r')$ can then be followed by an analogous manipulation of expansions (18)–(21). Because this term would normally vanish with use of the true Green function, and because the Green function that is actually used satisfies the right properties on a reference surface which, for not too large values of α and k , will not be so grossly different from the surface under study, one should expect that this term will be small in comparison with (24). Indeed, the dominant contribution at each order of η , within $\Delta\psi^{(1)}$, will come from the dominant contribution to $\psi^{(0)}$, that is, $f_0^{(0)}$. Consequently, in (27) I have used expression (26a) evaluated at $r = a$, and again made use of expansions (18), (21), (22) and the Taylor series for Q above, and that for $\delta Q \equiv \partial Q / \partial r$ below. In the expansion

$$\delta Q_{mp}(r, a + aF(\phi, z)) = \sum_n \frac{\eta^n}{n!} \delta Q_{mp}^{(n)}(r, a; \phi, \zeta),$$

the first three terms are

$$a \delta Q_{mp}^{(0)} = 4\pi \frac{S_0^{(mp)}(r) T_1^{(mp)}(a)}{A_{mp}} (\gamma_p a),$$

$$a^2 \delta Q_{mp}^{(1)} = 4\pi \frac{S_0^{(mp)}(r) T_2^{(mp)}(a)}{A_{mp}} (\gamma_p a)^2 \cos(kz') \cos(\phi')$$

and

$$a^3 \delta Q_{mp}^{(2)} = 4\pi \frac{(\gamma_p a)^2 S_0^{(mp)}(r)}{A_{mp}} [(\gamma_p a) T_3^{(mp)}(a) \cos^2(\phi') - T_2^{(mp)}(a) \sin^2(\phi')] \cos^2(kz').$$

With this procedure the correction terms that result are again those of the form of (23) with coefficient functions

$$f_1^{(0)}(r) = \frac{\sigma a}{\epsilon \epsilon_0} (\gamma_0 a) \frac{S_0^{(00)}(a) T_0^{(00)}(a) T_1^{(00)}(a) S_0^{(00)}(r)}{A_{00}^2}, \quad (28a)$$

$$f_1^{(1)}(r) = \frac{\sigma a}{\epsilon \epsilon_0} \frac{T_0^{(00)}(a) S_0^{(00)}(a) ((\gamma_1 a)^2 T_2^{(11)}(a) + (\gamma_1 a) T_1^{(11)}(a) - (1 + (ka)^2) T_0^{(11)}(a))}{A_{00} 4A_{11}} S_0^{(11)}(r) \quad (28b)$$

and, with

$$\Gamma_i = \frac{\sigma a T_0^{(00)}(a) S_0^{(00)}(a)}{\epsilon \epsilon_0 8A_{00}} (\gamma_i a),$$

$$\left. \begin{aligned} f_1^{(20)}(r) &= \Gamma_0 [(\gamma_0 a)^2 T_3^{(00)}(a) + (\gamma_0 a) T_2^{(00)}(a) - T_1^{(00)}(a)] S_0^{(00)}(r) / A_{00}, \\ f_1^{(21)}(r) &= \Gamma_0 [(\gamma_0 a)^2 T_3^{(02)}(a) + 3(\gamma_0 a) T_2^{(02)}(a) - 3T_1^{(02)}(a)] S_0^{(02)}(r) / A_{02}, \\ f_1^{(22)}(r) &= \Gamma_2 [(\gamma_2 a)^2 T_3^{(20)}(a) + (\gamma_2 a) T_2^{(20)}(a) - (1 + 4(ka)^2) T_1^{(20)}(a)] S_0^{(20)}(r) / A_{20}, \\ f_1^{(23)}(r) &= \Gamma_2 [(\gamma_2 a)^2 T_3^{(22)}(a) + 5(\gamma_2 a) T_2^{(22)}(a) - (3 + 4(ka)^2) T_1^{(22)}(a) \\ &\quad - 8(ka)^2 T_0^{(22)}(a)] S_0^{(22)}(r) / A_{22}. \end{aligned} \right\} \quad (28c)$$

Equations (26) and (28) together are the desired results. However, before embarking on a numerical description of their meaning, there are some comments worth making.

Firstly, it should have been noted that (26*a*) is not identical to the undisturbed solution, ψ_0 , quoted earlier. Now, it appears that (28*a*) presents a non-zero correction to the order unity term. The reason is that both (26*a*) and (28*d*) still retain some knowledge of the perturbation, through r_0 . If one were to set $r_0 = a$ in these, then $f_0^{(0)}$ would reduce to ψ_0 after an application of (12) to $T_0(a)$, and $f_1^{(0)}$ would vanish because of the $T_1(a)$ term. Clearly then (26*a*) is truly an order unity term while (28*a*) is implicitly of order η . This feature has the interpretation that (26) with (28) does not represent a true explicit power series solution of ψ in η (or α). This is actually advantageous because it effectively increases the radius of convergence of the expansion i.e. the expansion remains valid to larger values of η than it would otherwise for a straight power series (Morse & Feshbach 1953).

A second comment following from this concerns the question of sufficiency of using only the first iterate on the integral equation (and even that one approximate) as a correction. Although I have made no analytical effort to establish the validity of this approximation, a numerical comparison of the individual terms of $A\psi^{(1)}$ with those of $\psi^{(0)}$ does justify taking this step: corresponding terms of the correction are normally found to be at least an order of magnitude smaller than those of the latter. This is found to be the case under the numerical conditions shown below.

Finally, while the perturbation results have been quoted to second order in η , the numerical results presented in §4 include third order terms in both the zero order approximation and first order correction. (They have been excluded from the text for typographical convenience.) Use was made of recurrence properties, polynomial approximations and asymptotic expansions to get the most efficient and accurate evaluation of the hyperbolic Bessel functions of high orders and their derivatives (see Abramowitz & Stegun 1968).

5. Numerical calculations and discussions

The preceding analysis dealt with solving, by perturbation method, the modified Helmholtz equation subject to Neumann boundary conditions. However, the means used is not restricted to the present electrochemical context; other governing physical equations and boundary conditions are equally well tractable. With this more general philosophy in mind, I consider in the numerical illustrations below, the character of undulations which provide sufficient deviations to illustrate the extent of and direction in which they influence properties of the electrochemical system, while at the same time giving confidence to the convergence of the perturbation

expansion. The latter, incidently, has only been monitored numerically. For the purpose of illustration, I shall pay less heed to keeping with the assumption of small potentials required to justify using the linear PB equation. In fact, for curved geometries, under some reasonable set of conditions, the error consequently entertained is still small compared with the magnitude of the true potential (Verwey & Overbeek 1948). The dependences I therefore demonstrate are, at the least, qualitatively correct.

It is at once evident that undulation affects the electrostatic potential by increasing its magnitude, on average, throughout the entire region. Indeed, even for those chosen cases of salt concentration, (residual) surface charge density and cell radii for which the potential for the undeformed cylinder is low (i.e. $|\psi| \leq 25$ mV), it only remains low for very small values of η ($\eta \leq 0.1$). As was said, this has no relevance to the perturbation technique, but reflects only on the ethics of using the basic linear equation. It does mean that for more quantitative results one should eventually consider the more consistent use of the full nonlinear equation, for whose solution the same effects will remain.

There are many ways of incorporating flexible polyelectrolyte effects into double layer theories. Predominant among these is to treat them as either individual point (or small) charged particles connected by a phantom link (Valleau 1989; Åkesson *et al.* 1989; Miklavic *et al.* 1990; Woodward and Jönsson 1991) or as an 'ideal' continuum line of charge (Muthukumar 1987; van Opheusden 1988; Podgornik 1990, 1991, 1992). However, in view of our general findings, by treating the macromolecule on near equal footing to the mobile ions one is certain to overestimate the screening ability of the electrolyte: the predicted potential is lower than it should otherwise be. Because, to this order of theory, the mean potential about colloidal or biological macroions determines many of their solution related properties such as macromolecular conformation, ion distribution, ion binding, etc., estimations of magnitude based on these more ideal descriptions may be grossly in error.

As is often the case, ratios of characteristic length scales determine where and when idealized descriptions can be invoked. Certainly, at distances larger than the molecular size, 'contour strings' of charge may give equally adequate description on some qualitative level. However, it is more often the case that certain properties (e.g. macromolecular interaction as in the close packed DNA system) become interesting at distances of the order of the macromolecular size or smaller. At these distances there is then clearly a need to distinguish between mobile electrolytes and charged macromolecules. With 'point particle' and 'contour string of charge' descriptions becoming invalid at small macroion separations, what can be said of the other extreme? Two situations come to mind where ideality of shape ceases to be a valid assumption. One of these is with macromolecules, such as DNA, which are rough, but regular on a molecular scale. The other is in thermodynamic studies of reasonably stiff macromolecules, again such as DNA, or fluid-like macromolecular assemblies, like surfactant aggregates in hexagonal phase. These are usually (and inappropriately) considered as rigid (cylinders). A further feature (presently ignored) which arises naturally in the latter case, is that the stiffness (here measured by the wavenumber k) is generally solution dependent. As mentioned earlier, any general undulation consists of an infinite composition of Fourier modes. I have singled out for study one finite mode; its wavelength, λ , I deliberately wish to distinguish from any persistence length scale which can be (and is definitely so for DNA) very much larger.

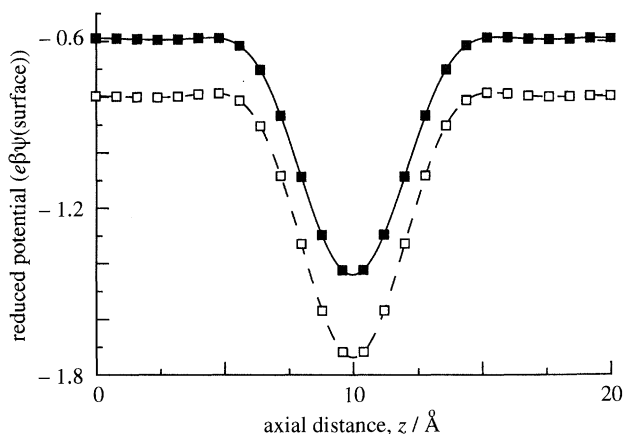


Figure 4. Electrostatic potential in reduced units ($e\beta\psi$) on the surface of the macroion, along the ray $\phi = 0$, as a function of axial distance, $a = 10 \text{ \AA}$, $\alpha = 2 \text{ \AA}$, $R = 50 \text{ \AA}$: $c_0 = 0.05 \text{ M}$ (\square), $c_0 = 0.1 \text{ M}$ (\blacksquare).

The need for any consideration of shape irregularities is to be qualified according to the characteristic length scales of each individual system. When the contour charge spacing, ζ , is much larger than the Debye length, i.e. $\kappa\zeta \gg 1$, then electrolyte screening is so efficient that the electrostatic contribution to the physical chemistry is negligible, and entropic (Helfrich & Harbich 1985) or mechanical (Manning 1989) considerations regarding undulations of neutral bodies alone dominate. For instances of extremely dilute electrolytes for which $\kappa\zeta \ll 1$ and yet $k/\kappa \ll 1$ with small amplitude, the hypothesis of a rigid straight cylinder is likely to be sufficient. But what then is the situation when both the wavelength and linear charge spacing is comparable to the Debye length? In the remaining discourse I consider effects where these ratios, $\kappa\zeta$ and k/κ , and L_B/ζ (where the Bjerrum length, $L_B = e^2\beta/(4\pi\epsilon\epsilon_0) = 7.14 \text{ \AA}$ in water at $25 \text{ }^\circ\text{C}$) are of order unity.

In the cases where $L_B k$ approaches unity, regions of negative curvature, i.e. where the charged surface is bent toward itself, certainly have a higher local potential than regions of positive curvature. This is exhibited in figure 4 which shows the potential on the macroion for one wavelength (here and below $\lambda = 20 \text{ \AA}$) of the surface along the ray, $\phi = 0$ (for $c_0 = 0.05 \text{ M}$, $\lambda_D/\lambda = 0.68$). The increase in magnitude matches the trough in the surface undulation. Reasoning from the dimensionless ratio k/κ , (or better λ_D/λ), this effect would be reduced by electrolyte screening, although this is not yet obvious with the increase in electrolyte to 0.1 M , shown in figure 4 ($\lambda_D/\lambda = 0.48$). From a biophysical viewpoint surface potentials are important in that they determine local electrolyte concentrations, including the distribution of potential-determining-ions, which play the special role of specific binders to dissociable surface groups (Ninham & Parsegian 1971); the increase in surface potential in these crevices would lead to an enhanced binding of these ions, above that predicted from rigid cylinder geometry (in a self-consistent sense).

Under any given set of conditions the effect of macroion curvature on the *shape* of the potential function is seen to diminish at larger distances from the surface; for the ray $\phi = 0$, this is shown in figure 5. However, it is significant that compared with the potential determined with the unperturbed geometry at equivalent radii, the *magnitude* remains consistently larger. At large enough distances, surface details are unimportant and similar values can be obtained using effective macroion properties.

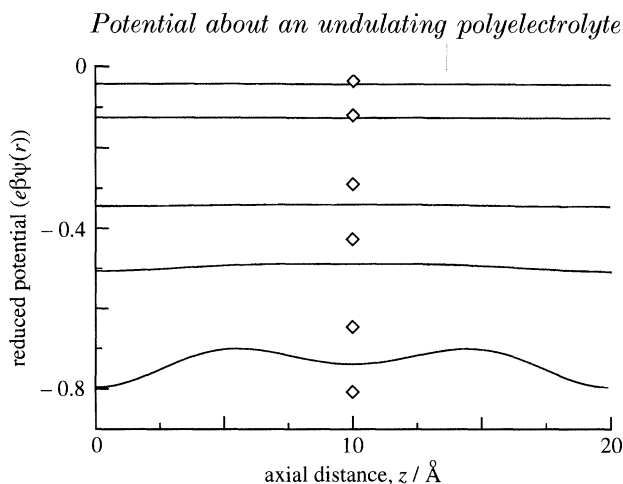


Figure 5. Electrostatic potential in reduced units ($e\beta\psi$) as a function of axial distance, $\phi = 0$. The different curves, from top to bottom, correspond to radii of 50, 30, 20, 16 and 12 Å. The accompanying symbols in the figure centre represent, for comparison at these same distances, the potential in the unperturbed condition. The additional, lowermost symbol gives the potential at the inner surface.

The unidirectional nature of our assumed undulation is ideal for study for it reveals the angular extent of the perturbation. This is demonstrated in figure 6 which particularizes to the potential at the cell wall. At $\phi = \pi/2$, the cylinder has zero curvature in the direction along the z axis. Here the potential value is least of all ϕ (for all $r \in [a, R]$), increasing on either side to maximum values at $\phi = 0$ and π . This increase toward 0 and π is accompanied by an increasing variation with z as r decreases in value. (There is no significant dependence on z at any r , for $\phi = \pi/2$; data not shown.) One may speculate that the maxima at 0 and π are due primarily to the fact that along these directions the undulation effectively brings the charged surface closer to the cell wall i.e. giving the appearance of a larger macroion. To some extent this is true; compare the value of $e\beta\psi(R)$ obtained with an unperturbed cylinder of radius 12 Å, -0.038 , with the ϕ -averaged value of -0.039 found with a cylinder of $a = 10$ Å and $\alpha = 2$ Å. Alternatively, the value of -0.038 could also be found with a rigid cylinder having an effectively higher surface charge.

Within this cell model of the electrical double layer it can be shown that the osmotic pressure due to the double layer, P_{osm} , is proportional to the total concentration of the mobile ions found at the cell wall, less the concentration of bulk electrolyte (Wennerström *et al.* 1982; Israelachvili 1991). This is an exact statistical mechanical result which carries over to the Gouy–Chapman approximation and is interpreted as the force per unit area per pair of macroions. Depending on the physical origin of the given undulation, whether arising from intrinsic surface roughness or from thermodynamic considerations of allowed conformation, this pressure should not be considered as the sole contribution to the total force. (For the latter possibility, another important term comes from the reduced entropy of confined undulations.) Regardless, it is still worthwhile to question what changes occur in P_{osm} when the surface is deformed. In the linear theory, P_{osm} is proportional to the square of the potential at the boundary, $P_{\text{osm}} = I\psi^2(\text{cell})/2kT$ (Verwey & Overbeek 1948; Israelachvili 1991). For a comparison with $\psi_0(R)$, the potential on the cell wall must be averaged over the polar angle, ϕ , $\langle \psi^2 \rangle_\phi$; note from figure 5 that the value is seen to be all but independent of z (the case for each ϕ). This comparison

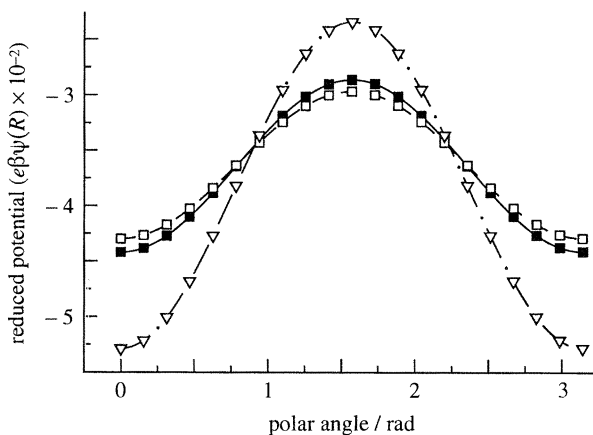


Figure 6. Electrostatic potential in reduced units ($e\beta\psi$) at the cell wall as a function of polar angle ϕ . Different curves correspond to the parameter sets $a = 10 \text{ \AA}$, $\alpha = 2 \text{ \AA}$, $R = 50 \text{ \AA}$ (\square), same a and α with $R = 25 \text{ \AA}$ (\blacksquare), $a = 10 \text{ \AA}$, $\alpha = 3 \text{ \AA}$ and $R = 50 \text{ \AA}$ (∇).

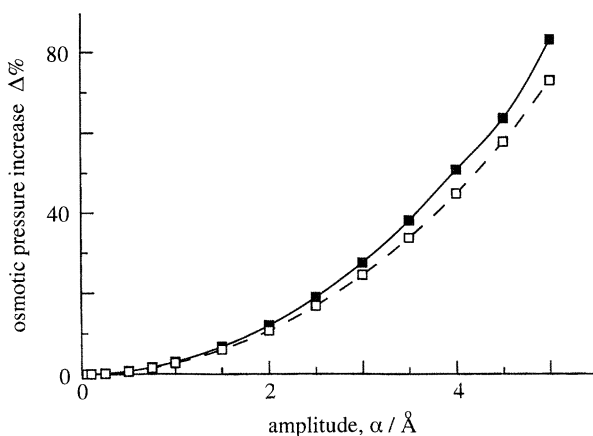


Figure 7. Relative percentage increase in osmotic pressure (ψ^2) in the undulating case (ϕ -averaged) over the unperturbed system. Data shown correspond to dimensions $a = 10 \text{ \AA}$, $R = 50 \text{ \AA}$ (\square) and $R = 25 \text{ \AA}$ (\blacksquare).

of osmotic pressure is plotted in figure 7 as a percentage relative difference in ψ^2 or equivalently P_{osm} , that is, $100(\langle\psi^2\rangle_\phi - \psi_0^2)/\psi_0^2$, as a function of undulation amplitude, for cell radii at 25 \AA and 50 \AA . By plotting the osmotic pressure in this relative way one eliminates, within linear theory, the dependence on the surface charge. The results shown are therefore valid for $f = 0.11$, 0.24 and 0.5 . For the nonlinear PB equation, the surface charge dependence would only be approximately eliminated.

From the figure it is clear that even with the rather low levels of undulation, to which one can reasonably refer as a perturbation, there is significant departure from the reference osmotic pressure. Moreover, the same extent of undulation, if present at smaller separations, leads to larger deviations. What figure 7 suggests is that the presence of any finite macroion undulation enhances the range of the electrostatic interaction between a pair of molecules. Not surprisingly, just as increasing electrolyte concentration reduces the double layer interaction at a finite separation, by reducing the extent of the double layer, so too does it reduce the osmotic pressure deviation at any given separation (data not shown). The feature of

enhanced electrostatic interaction has been pointed out as being responsible for the extended range of forces between aligned DNA molecules in univalent salt solutions (Podgornik *et al.* 1989). Although I sought a direct comparison with those measured forces using the model presented here, such was, unfortunately, not immediately forthcoming. By matching X-ray diffraction intensities to gaussian distributions, Podgornik *et al.* (1989) calculated the root mean square size of fluctuations of the DNA molecules about their equilibrium positions. They attributed these fluctuations strictly to undulations, the size of which was inherently related to the amplitude I used, α , and ranged between 5 and 10 Å. These values regrettably exceed the limitations of the perturbation approach. Despite this, the results are qualitatively consistent with their findings, and encourage further analysis in seeking to relate the model to these experiments.

So far I have treated the amplitude (and wavenumber too) as a parameter and studied the effects of undulation on double layer properties. As a final illustrative calculation I consider the contrary: to what extent does the double layer influence macromolecular undulation? One satisfactory way to estimate this extent is through statistical thermodynamic arguments. Here, one considers the double layer free energy which, for a constant charge surface, is given by the expression (Verwey & Overbeek 1948)

$$\int_{\text{surf}} dS \int_0^{\sigma} \psi_{\text{surf}}(\sigma') d\sigma'. \quad (29)$$

In the linear double layer model it is trivial to evaluate the surface charging integration, as the potential is linear in charge density; if one takes $r = a$ in the argument of the integrand, the surface integral is then also simple and one can get a leading estimate to (29). As a result of these integrations we get the expression

$$\frac{2\pi^2\sigma a}{k} \sum_{i=1}^2 (f_i^{(0)}(a) + \eta^2 f_i^{(20)}(a)).$$

In the analysis of degree of double layer influence on macromolecular undulation, one should consider the free energy difference between the charged undulating cylinder and the uncharged undulating cylinder. For the latter case, (29) vanishes and so this double layer free energy difference is (29) itself for the charged case alone. As a contribution to the total free energy of a system which permits a distribution of amplitudes, (29) must be balanced against the free energy change owing to restricted undulation, given in this context simply by $-kT \ln(\alpha/\alpha_0)$, where α_0 is the assumed amplitude of unrestrained undulation for an uncharged cylinder, whereas α is the operative amplitude. These two individual contributions are shown in figure 8 for a number of conditions of charge and cell size. For convenience, the double layer contribution is plotted as a free energy difference relative to the unperturbed, charged case, whose value for each condition is provided in the figure caption.

Like previous results this figure is self-explanatory. The double layer free energy contribution is least when the cylinder is straight whereas the undulation entropy is infinite at this extreme. In confirmation of what was already said, at low or zero surface charges (e.g. the case of $f = 0.11$) the total free energy is dominated by the undulation entropy term and the free energy minimum lies at the greatest undulation amplitude, $\alpha = \alpha_0 = 5$ Å. At finite σ , the minimum shifts to smaller values of α for any, even infinite, R (there being very little difference between the results using $R = 50$ Å and $R = 100$ Å): the greater the surface charge, the smaller

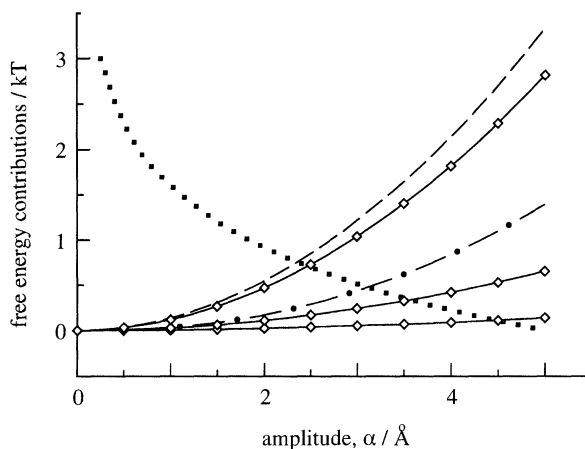


Figure 8. Contributions to the system free energy change, plotted as a function of α , of a charged undulating cylinder of amplitude α relative to an uncharged, undulating cylinder of amplitude $\alpha_0 = 5 \text{ \AA}$. The double layer contribution is shown relative to the straight cylinder free energy, F_{DL}^0 . Data shown correspond to cylinder dimension $a = 10 \text{ \AA}$. In order of increasing magnitude, the solid lines with superimposed open diamonds refer to: $f = 0.11$, $R = 50 \text{ \AA}$ ($F_{\text{DL}}^0 = 0.522 \text{ kT}$, $\alpha_{\text{min}} = 5 \text{ \AA}$); $f = 0.24$, $R = 50 \text{ \AA}$ ($F_{\text{DL}}^0 = 2.49 \text{ kT}$, $\alpha_{\text{min}} \lesssim 4.5 \text{ \AA}$); $f = 0.5$, $R = 50 \text{ \AA}$ ($F_{\text{DL}}^0 = 10.79 \text{ kT}$, $\alpha_{\text{min}} \gtrsim 2 \text{ \AA}$). The dot-dashed line relates to the latter case but at a concentration of 0.2 M ($F_{\text{DL}}^0 = 6.46 \text{ kT}$, $\alpha_{\text{min}} \approx 3.0 \text{ \AA}$). The dashed line corresponds to the condition $f = 0.5$, $R = 25 \text{ \AA}$, $c_0 = 0.05 \text{ M}$ ($F_{\text{DL}}^0 = 13.95 \text{ kT}$, $\alpha_{\text{min}} \lesssim 2 \text{ \AA}$). The undulation entropy $-kT \ln(\alpha/\alpha_0)$ is shown by the dotted line.

the amplitude for which the free energy is a minimum. However, it is impossible to imagine a (realistic) surface charge large enough to dominate over the diverging entropy term and so favour a completely straight cylinder. As the cell radius decreases, this ‘optimum’ amplitude (listed in the caption) also decreases. Clearly, the presence of a surface charge tends to ‘straighten out’ the cylinder, even when it is in isolation. Moreover, as the macromolecules are made to approach one another, it becomes unfavourable for their double layers to remain so extended and thus, significantly overlapping; equilibrium is re-established at a smaller amplitude. In circumstances such as these, when there is allowance for the amplitude to respond self-consistently to double layer changes, leading to these two contributions to the free energy, there will be an additional repulsive contribution to the net force (pressure), having its origin in the double layer induced constriction of undulations. I leave to future publication an explicit numerical study of this contribution.

6. Summary

The effect of macromolecular undulation on the electrostatic potential around a rod-like molecule is solved by perturbation technique. The Poisson–Boltzmann equation together with a constant charge boundary condition on the well-defined surface of an undulating cylinder is reformulated in integral equation form by use of Green’s theorem. The perturbation solution appropriate to the deformed boundary is found by approximating the Green function with one relevant to a reference, undeformed cylinder. Numerical results demonstrate that undulation causes significant deviations (increases) in such electrochemical properties as the double layer potential, osmotic pressure and free energy, from those relevant to a rigid cylinder. Measured intermolecular electrostatic forces acting in a condensed phase of close-packed DNA are consistent with expectations of this model. Comparison of

double layer free energy with undulation entropy show that electrostatics tend to suppress undulations, and that this suppression increases with increasing surface charge and decreasing intermolecular separation.

References

- Abramowitz, M. & Stegun, I. A. 1968 *Handbook of mathematical functions*, ch. 9. New York: Dover.
- Åkesson, T., Woodward, C. E. & Jönsson, B. 1989 Electric double layer forces in the presence of polyelectrolytes. *J. chem. Phys.* **91**, 2461–2469.
- Arfken, G. 1970 *Mathematical methods for physicists*, 2nd edn. New York: Academic Press.
- Bloomfield, V. A. 1991 Condensation of DNA by multivalent cations: considerations on mechanism. *Biopolymers* **31**, 1471–1481.
- Bloomfield, V. A., Wilson, R. W. & Rau, D. C. 1980 Polyelectrolyte effects by polyamines. *Biophys. Chem.* **11**, 339–343.
- Brenner, S. L. & Parsegian, V. A. 1974 A physical method for deriving the electrostatic interaction between rod-like polyions at all mutual angles. *Biophys. J.* **14**, 327–334.
- Carnie, S. L. & Torrie, G. 1984 Statistical mechanics of the electrical double layer. *Adv. chem. Phys.* **56**, 141–253.
- Chan, D. Y. C. & Chan, B. K. C. 1983 Electrical double layer interaction between spherical colloidal particles: An exact solution. *J. Colloid Interface Sci.* **92**, 281–283.
- Chau, F. P. & Eatock Taylor, R. 1992 Second-order wave diffraction by a vertical cylinder. *J. Fluid Mech.* **240**, 571–599.
- Chew, Y. T., Low, H. T., Wong, S. C. & Tan, K. T. 1992 An unsteady wake-source model for flow past an oscillating circular cylinder and its implications for Morison's equation. *J. Fluid Mech.* **240**, 627–650.
- Engström, S. & Wennerström, H. 1978 Ion condensation on planar surfaces. A solution of the Poisson–Boltzmann equation for two parallel charged plates. *J. phys. Chem.* **82**, 2711–2714.
- Fogden, A., Mitchell, D. J. & Ninham, B. W. 1990 Undulations of charged membranes. *Langmuir* **6**, 159–162.
- Fogden, A. & Ninham, B. W. 1991 The bending modulus of ionic lamellar phases. *Langmuir* **7**, 590–595.
- Gilson, M. K., Sharp, K. A. & Honig, B. H. 1987 Calculating the electrostatic potential of molecules in solution: Method and error assessment. *J. comp. Chem.* **9**, 327–335.
- Helfrich, W. & Harbich, W. 1985 Adhesion and cohesion of tubular vesicles. *Chem. Scr.* **25**, 32.
- Hill, T. L. 1956 *Statistical mechanics. Principles and selected applications*, reprint. New York: Dover.
- Israelachvili, J. I. 1991 *Intermolecular and surface forces*, 2nd edn. San Diego: Academic Press.
- Jönsson, B. & Wennerström, H. 1987 Phase equilibria in a three-component water-soap-alcohol system. A thermodynamic model. *J. phys. Chem.* **91**, 338–352.
- Kjellander, R. & Marcelja, S. 1988 Surface interactions in simple electrolytes. *J. Phys. France* **49**, 1009–1015.
- Maniatis, T., Venable, J. H. & Lerman, L. S. 1974 The structure of Ψ DNA. *J. molec. Biol.* **84**, 37–64.
- Manning, G. S. 1978 The molecular theory of polyelectrolyte solutions with applications to the electrostatic properties of polynucleotides. *Q. Rev. Biophys.* **11**, 179–246.
- Manning, G. S. 1989 Self attraction and natural curvature in null DNA. *J. biomol. Struct. Dyn.* **7**, 041–061.
- Marcus, R. A. 1955 Calculations of thermodynamic properties of polyelectrolytes. *J. chem. Phys.* **23**, 1057–1068.
- Miklavic, S. J., Woodward, C. E., Jönsson, B. & Åkesson, T. 1990 Interaction of charged surfaces with grafted polyelectrolytes: A Poisson–Boltzmann and Monte Carlo study. *Macromolecules* **23**, 4149–4157.

- Morse, P. M. & Feshbach, H. 1953 *Methods of theoretical physics*. New York: McGraw-Hill. (Properties of Green functions are given in Ch. 7, vol. 1; the perturbation method is discussed in ch. 9, vol. II.)
- Muthukumar, M. 1987 Adsorption of a polyelectrolyte chain to a charged surface. *J. chem. Phys.* **86**, 7230–7235.
- Ninham, B. W. & Parsegian, V. A. 1971 Electrostatic potential between surfaces bearing ionizable groups in ionic equilibrium with physiologic saline solutions. *J. theor. Biol.* **31**, 405–428.
- Odijk, T. 1983 On the statistics and dynamics of confined or entangled stiff polymers. *Macromolecules* **83**, 1340–1344.
- van Opheusden, J. H. J. 1988 Polyelectrolytes between two membranes or colloidal particles. *J. Phys. A* **21**, 2739–2751.
- Pashley, R. 1981 DLVO and hydration forces between mica surfaces in Li^+ , Na^+ , K^+ and Cs^+ electrolyte solutions: A correlation of double-layer and hydration forces with surface cation exchange properties. *J. Colloid Interface Sci.* **83**, 531–546.
- Podgornik, R. 1990 Forces and conformation of a polyelectrolyte chain between two charged walls. *Chem. Phys. Lett.* **174**, 191–198.
- Podgornik, R. 1991 Electrostatic forces between charged surfaces in the presence of a polyelectrolyte chain. *J. phys. Chem.* **95**, 5249–5255.
- Podgornik, R. 1992 Self-consistent theory for confined polyelectrolyte chains. *J. phys. Chem.* **96**, 884–896.
- Podgornik, R. & Parsegian, V. A. 1990 Molecular fluctuations in the packing of polymeric liquid crystals. *Macromolecules* **23**, 2265–2269.
- Podgornik, R., Rau, D. C. & Parsegian, V. A. 1989 The action of interhelical forces on the organization of DNA double helices: fluctuation-enhanced decay of electrostatic double-layer and hydration forces. *Macromolecules* **22**, 1780–1786.
- Rau, D. C., Lee, B. & Parsegian, V. A. 1984 Measurement of the repulsive force between polyelectrolyte molecules in ionic solution: hydration forces between parallel DNA double helices. *Proc. natn. Acad. Sci. USA* **81**, 2621–2625.
- Schellman, J. A. & Parthasarathy, N. 1984 X-ray diffraction studies on cation-collapsed DNA. *J. molec. Biol.* **175**, 313–329.
- Schellman, J. A. & Stigter, D. 1977 Electrical double layer, zeta potential and electrophoretic charge of double-stranded DNA. *Biopolymers* **16**, 1415–1434.
- Sengupta, A. K. & Papadopoulos, K. D. 1992 Electrostatic double layer interaction between two eccentric spherical surfaces. *J. Colloid Interface Sci.* **149**, 135–152.
- Stigter, D. 1978 A comparison of Manning's polyelectrolyte theory with the cylindrical Gouy model. *J. phys. Chem.* **14**, 1603–1606.
- Tanford, C. 1961 *Physical chemistry of macromolecules*, ch. 7. New York: Wiley.
- Valleau, J. P. 1989 Flexible polyelectrolyte in ionic solution: a Monte Carlo Study. *Chem. Phys.* **129**, 163–175.
- Verwey, E. J. W. & Overbeek, J. Th. G. 1948 *Theory of the stability of lyophobic colloids*. Amsterdam: Elsevier.
- Vlachy, V. & McQuarrie, D. A. 1985 A theory of cylindrical polyelectrolyte solutions. *J. chem. Phys.* **83**, 1927–1932.
- Watson, E. J. 1992 Slow oscillations of a circular cylinder or sphere in a viscous fluid. *Q. Jl Mech. appl. Math.* **45**, 263–275.
- Wennerström, H., Jönsson, B. & Linse, P. 1982 The cell model for polyelectrolyte systems. Exact statistical mechanical relations, Monte Carlo simulations and the Poisson–Boltzmann approximation. *J. chem. Phys.* **76**, 4665–4670.
- White, L. R. 1977 Approximate analytical solution of the Poisson–Boltzmann equation for a spherical colloidal particle. *J. chem. Soc. Faraday Trans. II* **73**, 577–596.
- Woodward, C. E. & Jönsson, B. 1991 Monte Carlo and mean field studies of a polyelectrolyte in a salt solution. *Chem. Phys.* **155**, 207–219.

Received 28 September 1992; revised 4 March 1993; accepted 17 May 1993